Milan Hanuš; Tomáš Berka; Marek Brandner; Roman Kužel; Aleš Matas
Three-dimensional numerical model of neutron flux in hex-Z geometry
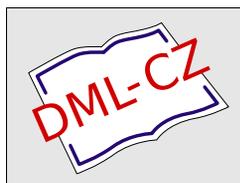
In: Jan Chleboun and Petr Přikryl and Karel Segeth and Tomáš Vejchodský (eds.): Programs and Algorithms of Numerical Mathematics, Proceedings of Seminar. Dolní Maxov, June 1-6, 2008. Institute of Mathematics AS CR, Prague, 2008. pp. 83–90.

Persistent URL: http://dml.cz/dmlcz/702860

THREE-DIMENSIONAL NUMERICAL MODEL OF NEUTRON FLUX IN HEX-Z GEOMETRY[*]

Milan Hanuš, Tomáš Berka, Marek Brandner, Roman Kužel, Aleš Matas

Abstract

We present a method for solving the equations of neutron transport with discretized energetic dependence and angular dependence approximated by the diffusion theory. We are interested in the stationary solution that characterizes neutron fluxes within the nuclear reactor core in an equilibrium state. We work with the VVER-1000 type core with hexagonal fuel assembly lattice and use a nodal method for numerical solution. The method effectively combines a whole-core coarse mesh calculation with a more detailed computation of fluxes based on the transverse integrated diffusion equations. By this approach, it achieves a good balance between accuracy and speed.

1. Multigroup diffusion theory

The set of steady-state neutron diffusion equations for G energy groups (the discrete ranges of neutron energies) can be written as follows:

$$\nabla \cdot \mathbf{j}^g(\mathbf{r}) + \Sigma_r^g(\mathbf{r})\phi^g(\mathbf{r}) = \sum_{\substack{g'=1 \\ g' \neq g}}^{G} \Sigma_s^{g' \to g}(\mathbf{r})\phi^{g'}(\mathbf{r}) + \frac{\chi^g}{k_{\text{eff}}} \sum_{g'=1}^{G} \nu\Sigma_f^{g'}(\mathbf{r})\phi^{g'}(\mathbf{r}). \qquad (1)$$

According to the usual notation,

$\mathbf{r} = (x, y, z)$	is the spatial variable,
$g = 1, 2, \ldots, G$	denotes the energy group,
ϕ^g	is the neutron flux in group g (density of neutrons),
$\mathbf{j}^g$	is the neutron current in group g (flow of neutrons in specific direction),
Σ_r^g	is the macroscopic removal cross section (characterizing losses of neutrons in given region and from group g),
$\Sigma_s^{g' \to g}$	is the macroscopic cross section characterizing scattering of neutrons from group g' into group g,
$\chi^g \nu\Sigma_f^{g'}$	characterizes the average number of neutrons that appear in group g due to fission induced by group g' neutrons,
k_{eff}	is the reactor critical number.

Each of the G equations in (1) describes local conservation of flux of neutrons having energy within the respective group. We specifically consider a two group model in

---

which the energy threshold separating the groups is chosen such that $\chi^1 = 1$, $\chi^2 = 0$, and $\Sigma_s^{2 \to 1} \equiv 0$ (for a physical explanation, see [3]).

Diffusion theory specifies the constitutive relation between neutron flux and neutron current by the Fick's law:

$$\mathbf{j}^g(\mathbf{r}) = -D^g(\mathbf{r})\nabla\phi^g(\mathbf{r}), \tag{2}$$

where D^g is the *diffusion coefficient*. Robin conditions apply on core boundary:

$$\gamma^g\phi^g(\mathbf{r}) - \mathbf{j}^g(\mathbf{r}) \cdot \mathbf{n} = 0, \quad \gamma^g = \frac{1 - \alpha^g}{2(1 + \alpha^g)}, \quad \mathbf{r} \in \partial\Omega, \tag{3}$$

where $\mathbf{n}$ denotes the unit outward normal to the boundary $\partial\Omega$ at point $\mathbf{r}$ and physical properties of core surroundings are captured by the *albedo* coefficient α^g.

There is only one value of parameter k_{eff} for which the boundary value problem (1)–(3) admits a physically realistic solution ([4]). Physicists refer to this value as to the *reactor critical number* since it shows the deviation of the steady state of the core from its critical state (i.e. one in which there is a perfect balance between production and losses of neutrons). Mathematically, it is the largest eigenvalue of the problem and the corresponding eigenfunction, uniquely determined up to a multiple, represents the physical flux solution.

2. Nodal method

A proven numerical method for solving problems arising from conservation laws is the finite volume method (FVM). In order to obtain a computationally efficient number of discrete equations, each finite volume (here called *node*) is identified with a section of a real fuel assembly loaded into the core lattice. Extents of the node equal to full assembly width and height h_z such that $H_z = Mh_z$, where H_z is the total height of the core, and M a chosen number of its horizontal cuts. Nodal geometry is displayed in Fig. 1 and has the following metric properties:

$$\ell = \frac{h}{\sqrt{3}}, \ F = \ell h_z, \ B = \frac{h^2\sqrt{3}}{2}, \ V = Bh_z,$$

where B is the area of the nodal base, F the area of the other faces and V the nodal volume. Denoting by N the number of assemblies and by $\mathcal{V}_i$ individual nodes, the core domain is thus discretized as $\Omega = \bigcup_{i=1}^{NM} \mathcal{V}_i$. To each node we further associate a local coordinate system by unit vectors $\mathbf{e}_x$, $\mathbf{e}_u$, $\mathbf{e}_v$, $\mathbf{e}_z$ as shown in Fig. 1. Finally, we refer by symbols $\mathcal{V}_{i+\xi}$ and $\mathcal{V}_{i-\xi}$ to nodes adjacent to the reference node $\mathcal{V}_i$ to the right and left, respectively, with respect to coordinate direction $\xi \in \{x, u, v, z\}$. Their common face is denoted by $\mathcal{F}_{i,\xi\pm}$, i.e. $\mathcal{F}_{i,\xi\pm} = \mathcal{V}_i \cap \mathcal{V}_{i\pm\xi}$.

The equation expressing the local balance of group g of neutrons in node $\mathcal{V}_i$ can be formally obtained by integrating eq. (1) over $\mathcal{V}_i$, dividing by its volume and using the divergence theorem (for a rigorous derivation, see e.g. [3]):
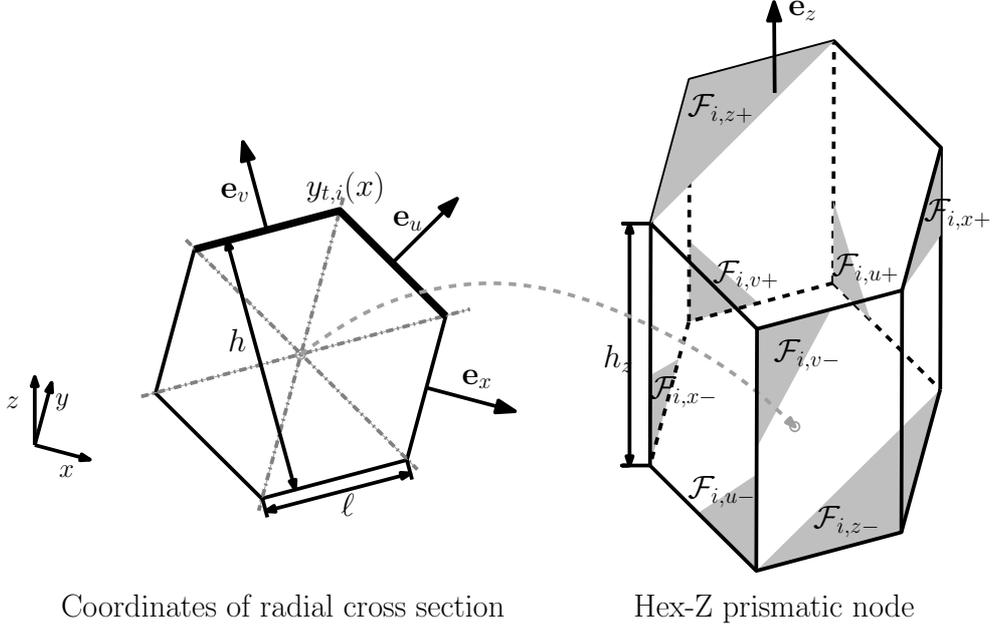
Coordinates of radial cross section   Hex-Z prismatic node

Fig. 1: *Geometry of node $\mathcal{V}_i$.*

$$\frac{F}{V}\sum_{\xi\in\{x,u,v\}}\left(\bar{\bar{\jmath}}^g_{i,\xi+}-\bar{\bar{\jmath}}^g_{i,\xi-}\right)+\frac{B}{V}\left(\bar{\bar{\jmath}}^g_{i,z+}-\bar{\bar{\jmath}}^g_{i,z-}\right)+\Sigma^g_{i,r}\bar{\bar{\bar{\phi}}}^g_i=\sum_{\substack{g'=1\\g'\neq g}}^{2}\Sigma^{g'\to g}_{i,s}\bar{\bar{\bar{\phi}}}^{g'}_i+\frac{\chi^g}{k_{\text{eff}}}\sum_{g'=1}^{2}\nu\Sigma^{g'}_{i,f}\bar{\bar{\bar{\phi}}}^{g'}_i. \quad (4)$$

The discrete unknowns in this equation are the *node-averaged neutron fluxes*:

$$\bar{\bar{\bar{\phi}}}^g_i:=\frac{1}{V}\iiint_{\mathcal{V}_i}\phi^g(\mathbf{r})\,\mathrm{d}\mathbf{r}\,,$$

and the 6 *face-averaged radial* and 2 *base-averaged axial neutron currents*, respectively:

$$\bar{\bar{\jmath}}^g_{i,\xi\pm}:=\frac{1}{F}\iint_{\mathcal{F}_{i,\xi\pm}}\mathbf{j}^g(\mathbf{r})\cdot\mathbf{e}_\xi\,\mathrm{d}\mathcal{F}\,,\ \text{for}\ \xi\in\{x,u,v\},\ \text{and}\ \bar{\bar{\jmath}}^g_{i,z\pm}:=\frac{1}{B}\iint_{\mathcal{F}_{i,z\pm}}\mathbf{j}^g(\mathbf{r})\cdot\mathbf{e}_z\,\mathrm{d}\mathcal{F}\,.$$

We assume that physical properties of each fuel assembly are homogeneous, thus justifying the spatially constant Σ terms.

2.1. Coarse mesh, finite difference (CMFD) approximation

The standard FVM relation between discrete flux and current is obtained by replacing the flux derivative in eq. (2) by finite difference (FD) expressions and is thus usable only for small nodal sizes. The modification appropriate for relatively large nodal sizes characteristic for efficient reactor core models is called *nodal method.*

It is based on the following approximation of discrete average currents at interfaces $\mathcal{F}_{i,\xi+}$ and $\mathcal{F}_{i,\xi-}$, respectively:

$$
\begin{aligned}
\bar{\bar{J}}_{i,\xi+}^g &:= -D_{i,\xi+}^g\big(\bar{\bar{\bar{\Phi}}}_{i+\xi}^g - \bar{\bar{\bar{\Phi}}}_i^g\big) + {}^{\mathrm{C}}D_{i,\xi+}^g\big(\bar{\bar{\bar{\Phi}}}_i^g + \bar{\bar{\bar{\Phi}}}_{i+\xi}^g\big), \quad D_{i,\xi+}^g := \frac{2D_i^g D_{i+\xi}^g}{h_\xi\big(D_i^g + D_{i+\xi}^g\big)}, \\
\bar{\bar{J}}_{i,\xi-}^g &:= -D_{i,\xi-}^g\big(\bar{\bar{\bar{\Phi}}}_i^g - \bar{\bar{\bar{\Phi}}}_{i-\xi}^g\big) + {}^{\mathrm{C}}D_{i,\xi-}^g\big(\bar{\bar{\bar{\Phi}}}_{i-\xi}^g + \bar{\bar{\bar{\Phi}}}_i^g\big), \quad D_{i,\xi-}^g := \frac{2D_{i-\xi}^g D_i^g}{h_\xi\big(D_{i-\xi}^g + D_i^g\big)}
\end{aligned} \tag{5}
$$

(as a convention, capital letters will denote approximations of corresponding lower-case quantities, e.g. $\bar{\bar{J}}_{i,\xi+}^g \approx \bar{\bar{j}}_{i,\xi+}^g$). At core boundary, i.e. if $\mathcal{F}_{i,\xi\pm} \subset \partial\Omega$, expressions obtained by analogous discretization of the boundary condition (3) are used instead:

$$
\bar{\bar{J}}_{i,\xi\pm}^g := D_{i,\xi\pm}^g \bar{\bar{\bar{\Phi}}}_i^g + {}^{\mathrm{C}}D_{i,\xi\pm}^g \bar{\bar{\bar{\Phi}}}_i^g, \quad D_{i,\xi\pm}^g := \pm\frac{2D_i^g \gamma_\xi}{h_\xi \gamma_\xi + 2D_i^g}, \quad \gamma_\xi^g := \frac{1 - \alpha_\xi^g}{2(1 + \alpha_\xi^g)}. \tag{6}
$$

Different albedoes are defined for radial and axial boundaries which results in $\gamma_\xi = \gamma_{\mathrm{rad}}$ for $\xi \in \{x, u, v\}$ and $\gamma_z = \gamma_{\mathrm{ax}}$. Also note that $h_x = h_u = h_v \equiv h$.

This so called *CMFD approximation* alters the standard FD expressions by adding a term containing the *coupling correction factor* ${}^{\mathrm{C}}D^g$. This factor accounts for the coarse mesh spacing by forcing the rough estimate of current to match a more accurate value obtained by some appropriate refining calculation. We describe one possible method for getting such higher-quality solution in Section 2.2.

By inserting the CMFD expressions (5) or (6) into eq. (4), we obtain the following numerical approximation of the discrete balance relation for node $\mathcal{V}_i$ and group g:

$$
\frac{2}{3}\sum_{\xi\in\{x,u,v\}} \bar{\bar{L}}_{i,\xi}^g + \bar{\bar{L}}_{i,z}^g + \Sigma_{i,r}^g \bar{\bar{\bar{\Phi}}}_i^g = \sum_{\substack{g'=1 \\ g'\neq g}}^2 \Sigma_{i,s}^{g'\to g} \bar{\bar{\bar{\Phi}}}_i^{g'} + \frac{\chi^g}{K_{\mathrm{eff}}}\sum_{g'=1}^2 \nu\Sigma_{i,f}^{g'} \bar{\bar{\bar{\Phi}}}_i^{g'}, \tag{7}
$$

where $\bar{\bar{L}}_{i,\xi}^g := \frac{\bar{\bar{J}}_{i,\xi+}^g - \bar{\bar{J}}_{i,\xi-}^g}{h_\xi}$ is the *neutron leakage* term expressing the average net neutron current through faces orthogonal to direction ξ. Using the lexicographic ordering of nodes inside the core, a matrix formulation follows:

$$
\underbrace{\begin{bmatrix} \mathbf{L}^1 + {}^{\mathrm{C}}\mathbf{D}^1 + \boldsymbol{\Sigma}_r^1 & \mathbf{0} \\ -\boldsymbol{\Sigma}_s^{1-2} & \mathbf{L}^2 + {}^{\mathrm{C}}\mathbf{D}^2 + \boldsymbol{\Sigma}_r^2 \end{bmatrix}}_{\mathbf{M}} \cdot \underbrace{\begin{bmatrix} \bar{\bar{\bar{\Phi}}}^1 \\ \bar{\bar{\bar{\Phi}}}^2 \end{bmatrix}}_{\bar{\bar{\bar{\Phi}}}} = \frac{1}{K_{\mathrm{eff}}} \underbrace{\begin{bmatrix} \nu\boldsymbol{\Sigma}_f^1 & \nu\boldsymbol{\Sigma}_f^2 \\ \mathbf{0} & \mathbf{0} \end{bmatrix}}_{\mathbf{F}} \cdot \underbrace{\begin{bmatrix} \bar{\bar{\bar{\Phi}}}^1 \\ \bar{\bar{\bar{\Phi}}}^2 \end{bmatrix}}_{\bar{\bar{\bar{\Phi}}}}, \tag{8}
$$

where $\bar{\bar{\bar{\Phi}}}^g$ is a vector of NM average fluxes in group g, $\mathbf{L}^g$ and ${}^{\mathrm{C}}\mathbf{D}^g$ are matrices of finite-difference and correction factors, and $\boldsymbol{\Sigma}_r^g$, $\boldsymbol{\Sigma}_f^g$, $\boldsymbol{\Sigma}_s^{1-2}$ are diagonal matrices of reaction cross sections. All matrices are sparse of order NM.

Being a discrete analogue of the eigenvalue problem (1)–(3) for the neutron diffusion operator, eq. (8) expectedly constitutes a matrix eigenvalue problem. We also

expect the same behaviour of its eigensolutions which allows us to use the standard power method for calculating the largest eigenvalue K_{eff} and the eigenvector $\bar{\bar{\bar{\mathbf{\Phi}}}}^g$ of average nodal fluxes. The actual implementation of this so called *CMFD iteration* consists of two levels – the outer *source* iteration advancing the eigenvalue approximation as in the classical power method and the inner calculation of the fluxes vector according to eq. (8) with a fixed right-hand side.

2.2. Refinement of the CMFD approximation

After a few eigenvalue updates, the CMFD iteration is interrupted to refine the iteration matrix by determining new correction factors. For this purpose, one-dimensional diffusion equations are formed for each direction $\mathbf{e}_\xi$ by performing the transverse integration procedure. For a chosen node $\mathcal{V}_i$ and any of the radial directions, this amounts to integrating eq. (1) over a section slicing through the node orthogonally to the given direction. To illustrate the procedure for the x-direction, we integrate the 'flux version' of the equation (obtained by inserting (2) into eq. (1)) along the y and z axes and make an average over the cross-section area. This yields the following 1D diffusion equation (group index will be omitted in this section):

$$-D_i \frac{\mathrm{d}^2 \bar{\bar{\phi}}_i(x)}{\mathrm{d}x^2} + \Sigma_{i,r} \bar{\bar{\phi}}_i(x) = \bar{\bar{s}}_i(x) - \bar{\bar{l}}_i(x) \tag{9}$$

for the unknown *transverse-averaged flux*:

$$\bar{\bar{\phi}}_i(x) := \frac{1}{h_z} \int_{-h_z/2}^{h_z/2} \frac{1}{2y_i^t(x)} \int_{-y_i^t(x)}^{y_i^t(x)} \phi(x,y,z) \, \mathrm{d}y \, \mathrm{d}z \,, \tag{10}$$

where $y_i^t(x) = 1/\sqrt{3}(h - |x|)$ represents the radial transverse boundary of the node (the bold line in Fig. 1). The source term $\bar{\bar{s}}_i(x)$ abbreviates the transverse-averaged right-hand side of eq. (1), whereas the *transverse leakage term* $\bar{\bar{l}}_i(x)$ basically contains the normal components of neutron currents through transverse boundary faces $\mathcal{F}_{i,u\pm}$, $\mathcal{F}_{i,v\pm}$ and $\mathcal{F}_{i,z\pm}$. Since the CMFD solution provides only the average surface currents and their spatial dependence is not known until the transverse integrated equations in the remaining directions are solved, we need to approximate the transverse currents shapes to establish $\bar{\bar{l}}_i(x)$. By inserting (10) into eq. (9) and denoting the cusp of the boundary function $y_i^t(x)$, it becomes clear, however, that we also need to cope with the singularities that arise in $\bar{\bar{l}}_i(x)$ due to the differentiation of $y_i^t(x)$ and which form the other part of the transverse leakage term.

There are currently two approaches to the problem of hexagonal transverse leakage approximation investigated at our department. In the first, originally described in [1], the hexagonal problem is conformally mapped to a rectangular one, effectively eliminating the source of the singularities. In the other, invented by M.R. Wagner ([5]) and followed in this paper, singular terms in $\bar{\bar{l}}_i(x)$ are neglected. This gives the approximation $\bar{\bar{L}}_i(x) \approx \bar{\bar{l}}_i(x)$ which transforms eq. (9) into an approximate

equation. We then seek its solution $\bar{\bar{\Phi}}_i(x) \approx \bar{\bar{\phi}}_i(x)$ so that the 1D problem remains consistent with the original 3D one in the sense of preserving the nodal averages of approximated quantities:

$$\frac{1}{V} \int_{-h/2}^{h/2} 2y_i^t(x) h_z \bar{\bar{\Phi}}_i(x) \, \mathrm{d}x = \bar{\bar{\bar{\Phi}}}_i, \quad \frac{1}{V} \int_{-h/2}^{h/2} 2y_i^t(x) h_z \bar{\bar{L}}_i(x) \, \mathrm{d}x = \bar{\bar{\bar{L}}}_i^{yz}. \quad (11)$$

Average nodal leakage $\bar{\bar{\bar{L}}}_i^{yz}$ through faces intersecting the y and z axes is obtained by integrating the 1D diffusion equation from $-h/2$ to $h/2$ and comparing the result with the original 3D eq. (7). This leads to:

$$\bar{\bar{\bar{L}}}_i^{yz} := \frac{2}{3}(\bar{\bar{\bar{L}}}_{i,u} + \bar{\bar{\bar{L}}}_{i,v}) - \frac{1}{3}\bar{\bar{\bar{L}}}_{i,x} + \bar{\bar{\bar{L}}}_{i,z}. \quad (12)$$

It is reasonable to assume that spatial variation of the transverse leakage function $\bar{\bar{L}}_i(x)$ is determined by the leakages through the transverse boundaries, i.e.

$$\bar{\bar{L}}_i(x) = f_i^{t,rad}(x) - \frac{1}{3}\bar{\bar{\bar{L}}}_{i,x}, \quad (13)$$

where the shape function $f_i^{t,rad}(x)$ involves only $\bar{\bar{\bar{L}}}_{i,u}$, $\bar{\bar{\bar{L}}}_{i,v}$, $\bar{\bar{\bar{L}}}_{i,z}$ and the second term ensures the consistency, whatever singularities the exact function $\bar{\bar{l}}_i(x)$ may contain.

Transverse integration in the axial direction leads to a z-direction diffusion equation formally identical to eq. (9). The transverse-averaged flux is now defined as

$$\bar{\bar{\phi}}_i(z) := \frac{1}{B} \int_{-h/2}^{h/2} \int_{-y_i^t(x)}^{y_i^t(x)} \phi(x,y,z) \, \mathrm{d}y \, \mathrm{d}x$$

and hence the transverse leakage term comprises only currents through faces orthogonal to the horizontal cross-section of the node. The approximate neutron balance relation may then be formally obtained by replacing $\bar{\bar{\phi}}_i(z)$ and $\bar{\bar{l}}_i(z)$ in the axial version of eq. (9) with their approximations $\bar{\bar{\Phi}}_i(z)$ and $\bar{\bar{L}}_i(z)$, respectively. They are again constructed so as to make the 1D and 3D equations consistent:

$$\frac{1}{h_z} \int_{-h_z/2}^{h_z/2} \bar{\bar{\Phi}}_i(z) \, \mathrm{d}z = \bar{\bar{\bar{\Phi}}}_i, \quad \frac{1}{h_z} \int_{-h_z/2}^{h_z/2} \bar{\bar{L}}_i(z) \, \mathrm{d}z = \bar{\bar{\bar{L}}}_i^{xy} := \frac{2}{3} \sum_{\xi \in \{x,u,v\}} \bar{\bar{\bar{L}}}_{i,\xi} \quad (14)$$

Introducing the axial transverse profile function $f_i^{t,ax}(z)$ correspondingly to the radial case, we have $\bar{\bar{L}}_i(z) = f_i^{t,ax}(z)$ since there are no singularities in $\bar{\bar{l}}_i(z)$.

The simplest transverse profile function can be obtained by assuming a non-varying (*flat*) transverse leakage throughout the node, i.e. $f_i^{t,rad}(x) := \frac{2}{3}(\bar{\bar{\bar{L}}}_{i,u} + \bar{\bar{\bar{L}}}_{i,v}) + \bar{\bar{\bar{L}}}_{i,z}$ and $f_i^{t,ax}(z) := \bar{\bar{\bar{L}}}_i^{xy}$. This approximation can be improved by taking into account the transverse leakages of two adjacent nodes $\mathcal{V}_{i-x}$, $\mathcal{V}_{i+x}$ and considering the consistency conditions for $\bar{\bar{L}}_i(x)$ also in their respective intervals. Assuming a parabolic transverse leakage profile, these three conditions form a system of three algebraic equations for the parabola's coefficients. Restriction of the resulting polynomial to $[-h/2, h/2]$ then defines $f_i^{t,rad}(x)$. An analogous approach is used in the axial direction.

88

2.3. Solution procedure

Equations (9) are cast into a group-matrix form and solved for both groups simultaneously by a semi-analytic method, first in the radial directions. Right-hand sides of the equations are defined using the results of the latest finished CMFD iteration. The algorithm sweeps through all pairs of nodes in given radial plane and direction, using the interface flux and current continuity conditions and the weighted residual method to solve the approximate 1D diffusion equations. The solution is expressed in terms of the face-averaged radial currents. Once these currents are known for all nodes in all planes, they are used to specify the transverse leakage term on the right-hand sides of the z-direction equations. Base-averaged axial currents can then be determined in the same manner (see [3] or [2] for further details). CMFD correction factors are finally obtained from eq. (5), (6) by equating their right-hand sides to the high-accuracy currents from the radial and axial sweeps. This completes the two-node subdomains solution and specifies new elements of the ${}^C\mathbf{D}^g$ matrices, which in turn update the CMFD iteration matrix $\mathbf{M}$ (cf. eq. (8)). Another few CMFD iterations advancing the eigensolution are then performed and again followed by refinement sweeps. This procedure is repeated as long as the CMFD matrix changes considerably after each refining step.

The converged vector of node average fluxes may be analysed in various ways. Specifically for the benchmark problem presented in Section 3, we need the average nodal powers normalized to the average power of the whole core:

$$\bar{\bar{\bar{P}}}_i := \frac{1}{P}\big(\nu\Sigma^1_{i,f}\bar{\bar{\bar{\Phi}}}^1_i + \nu\Sigma^2_{i,f}\bar{\bar{\bar{\Phi}}}^2_i\big),\ i = 1, 2, \ldots, NM;\ P := \frac{1}{NM}\sum_{j=1}^{NM}\big(\nu\Sigma^1_{j,f}\bar{\bar{\bar{\Phi}}}^1_j + \nu\Sigma^2_{j,f}\bar{\bar{\bar{\Phi}}}^2_j\big),$$

and the axial offset, defined as the percentage difference between the average power generated in the upper and the lower halves of the core.

3. Numerical tests and conclusions

We tested the developed method by "Benchmark problem no. 6" from [1]. The investigated VVER-1000 type core is 200 cm high and has 163 fuel assemblies with radial pitch of 23.6 cm. As in [1], we divided the core into 10 axial layers, i.e. the height of each node was $h_z = 20$ cm. The calculation was finished by convergence of correction factors, indicated in step s by $\left\|{}^C\mathbf{D}^{(s)} - {}^C\mathbf{D}^{(s-1)}\right\|_\infty < \varepsilon = 10^{-6}$.

Table 1 shows deviations of the results from those of a fine-mesh finite-difference method DIF3D (reference is given in [1]), measured as the maximum and root mean square errors in average nodal powers ($\Delta\bar{\bar{\bar{P}}}_{max}$ and $\Delta\bar{\bar{\bar{P}}}_{rms}$, resp.), error in axial offset (ΔAO), and error in critical number (ΔK_{eff}). The table compares four versions of the method based on four combinations of transverse leakage approximation with two versions of the ANC code presented in [1]. ANC-HW uses Wagner's approach to hexagonal transverse leakage (as do we in this paper) while ANC-HM uses the conformal mapping technique. Neither of the ANC methods uses CMFD to advance

$Method^{\dagger}$	$\Delta\bar{\bar{P}}_{max}$ [%]	$\Delta\bar{\bar{P}}_{rms}$ [%]	ΔAO [%]	ΔK_{eff} [pcm=10^{-5}]
rFaF	10.3	4.5	-1.10	156.9
rFaQ	10.1	4.4	-1.15	138.1
rQaF	4.9	1.7	-0.41	7.6
rQaQ	4.7	1.7	-0.48	-12.3
ANC-HW	12.0	N/A‡	1.17	113.0
ANC-HM	0.9	N/A‡	0.07	13.0

$^{\dagger)}$ r ...approx. of $f_i^{t,rad}$, a ...approx. of $f_i^{t,ax}$; F ...flat, Q ...quadratic

$^{\ddagger)}$ result was not available

Tab. 1: *Benchmark results.*

the global solution, however, and both assume different transverse leakage shapes than do we in our four schemes.

The results indicate that it is the transverse leakage approximation used in radial direction that mostly determines the accuracy of results. Quadratic approximation proves to be superior to the flat one, although when the latter is used in the axial direction (in which the nodes are rectangular), it may give somewhat better core-wise average results. This results in a slightly better axial offset characterization and, in the case of sufficiently low maximum flux errors, also in a better critical number estimate. Either version of our method performs better than the ANC-HW method, which was developed under the same assumptions based on original Wagner's ideas, except for the transverse leakage profile. However, the superior accuracy of the conformal mapping technique for flux prediction still remains unmatched. This suggests that further research into integration of the CMFD and conformal mapping methods could yield fruitful results.

References

[1] Y.A. Chao, Y.A. Shatilla: *Conformal mapping and hexagonal nodal methods – II.* Nucl. Sci. Eng. **121** (1995), 210–225.

[2] X.D. Fu, N.Z. Cho: *Nonlinear analytic and semi-analytic nodal methods for multigroup neutron diffusion calculations.* J. Nucl. Sci. Technol. (Tokyo, Jpn.) **39** (2002), 1015–1025.

[3] M. Hanuš: *Numerical modelling of neutron flux in nuclear reactors.* Faculty of Applied Sciences, University of West Bohemia in Pilsen 2007. Bachelor's Thesis.

[4] E.L. Wachspress: *Iterative solution of elliptic systems and applications to the neutron diffusion equations of reactor physics.* Prentice-Hall, Inc., Englewood Cliffs, NJ, 1966.

[5] M.R. Wagner: *Three-dimensional nodal diffusion and transport theory methods for hexagonal-z geometry.* Nucl. Sci. Eng. **103** (1989), 377–391.